《연구논문》 Hankook Kwanghak Hoeji, Volume 15, Number 4, August 2004

소형 위성용 고해상도 광학카메라의 광학정렬

김도형† · 최영완 · 강명석 · 김이을

㈜쎄트렉아이

㊒ 305-811 대전 유성구 전민동 461-26번지

양호순

한국표준과학연구원

㊒ 305-600 대전 유성구 도룡동 1번지

(2004년 5월 13일 받음, 2004년 7월 5일 수정본 받음)

인공위성용 지구관측 카메라나 우주관측 망원경에는 크기와 무게의 제약 때문에 Cassegrain 방식의 망원경이 많이 쓰인다. 이와 같은 우주광학계의 성공적인 임무수행을 위해서는 망원경부의 정밀한 광학정렬이 매우 중요하다. 본 논문에서는 정렬 정밀도에 따른 Cassegrain 방식 망원경부의 광학정렬 방법 중, 간섭무늬를 이용한 방법, 파면오차를 이용한 방법, 역최적화 광학정렬 방법 등을 모사를 통해 제시하고, 현재 개발 중인 구경 300 mm급 소형 위성용 카메라에 적용한 광학정렬 실험 결과를 정리한다.

주제어 : space optics, telescopes, alignment.

I. Introduction

Cassegrain design is often used for spaceborne telescopes due to the compactness of the design, as instrument volume and mass are critical for space instruments. The importance of precision optical alignment of such a telescope cannot be too emphasized. Optical alignment of a Cassegrain telescope can be typically done by 1) visual inspection with an alignment telescope, 2) inspection of the spot image or telescope interferograms, and 3) reverse-optimzation alignment method, in the order of increasing precision of alignment accuracy. The required alignment methods are determined by the alignment tolerances, which are influenced by the wavelengths, and tolerances other than alignment tolerances. The telescope for a space optical camera often needs highest alignment precision, but some ground based IR telescopes do not require high alignment tolerances. Telescopes with higher alignment tolerances often need all the above alignment methods from coarse to fine alignment stages, but it has been reported that an IR (wv=2.4 microns) telescope of 600 mm diameter has been completely aligned with visual inspection only.[1] After a coarse alignment stage, spot image inspection, or interferogram inspection method is used for finer alignment. Spot image inspection is also called "star test," and it is often used for larger telescopes where an interferometer cannot be installed for a double-pass setup.[2] Interferogram inspection method can be used for smaller telescopes, which can be tested in a laboratory. The current state-of-the-art alignment method is reverse-optimized alignment, or computer-aided alignment method.[3] The advantage of this method is that it gives the alignment error quantitatively, and this can be useful for a numerically controlled alignment process.

The alignment methods described above have been applied on the Qualification Model (QM) of Medium-sized Aperture Camera (MAC) telescope. Developed as a push-broom type high-resolution camera, the telescope has one panchromatic and four multispectral channels. The panchromatic channel has 2.5 m, and multispectral channels have 5 m of ground sampling distances at a nominal altitude of 685 km. The 300 mm-aperture modified Ritchey-Chrétien telescope contains two aspheric mirrors and two spherical correction lenses. The telescope has +/-1 deg of field of view, and 2 m of effective focal length. With a philosophy of building a simple and cost-effective camera, the mirrors incorporate no light-weighting schemes, and the linear CCDs are mounted on a single PCB with no beam splitting optics. MAC is the main payload of RazakSAT to be launched in 2005.[4] MAC and RazakSAT program was initiated as an international research and development collaboration program between Satrec Initiative of Korea and Astronautic Technology Sdn. Bhd. of Malaysia. RazakSAT is a 180 kg satellite including MAC, designed to provide high-resolution imagery of 20 km swath width on a near equatorial orbit (NEqO).[5] The mission objective is to demonstrate the capability of a small high-resolution remote

† E-mail: edk@satreci.com

sensing satellite system on a near equatorial orbit.

This paper describes the three alignment methods established in the course of MAC QM telescope development with the simulation and experiment results. Interferogram inspection method named Fringe Density Balancing Method (FDBM), and wavefront inspection method called OPD Balancing Method (OBM) are simulated on the telescope design and a reverse-optimization method is reviewed with the experiment results.

II. Fringe Density Balancing Method and OPD Balancing Method

Based on the tolerance analyses of MAC telescope, five secondary mirror movements were used to align the Cassegrain telescope. The five degrees of freedom include X&Y decenters, X&Y tilts, and Z displacement as shown in Figure 1 (a). All other alignment tolerances were found to be less sensitive and they could be assembled with mechanical tolerances. Figure 1 (b) shows the 5-DOF mount for the secondary mirror. The translation range was +/-10 mm and angular range was +/-7 deg, with minimum reading of 0.01 mm and 30arcsec.

(a)

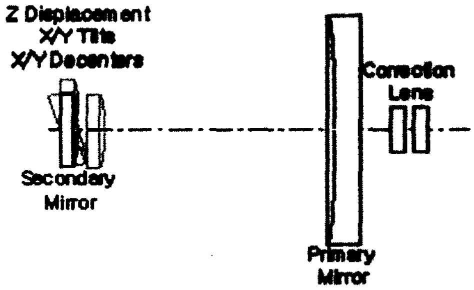

(b)

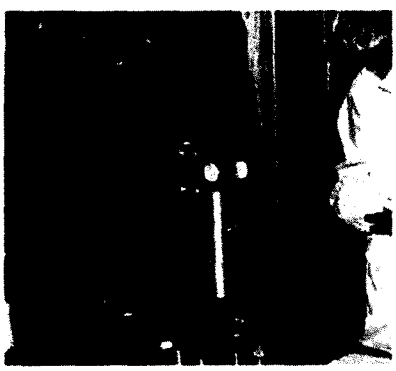

Figure 1. Alignment movements and 5-DOF mount for the secondary mirror of MAC.

Firstly, the effect of each (mis)alignment component on Zernike coefficients of the telescope was checked. Table 1 shows that the decenter and tilt of the secondary mirror mainly influence the Zernike tilt and coma terms. Astigmatism term is also influenced by less noticeably. The interferograms were produced in Code V, but in the actual experiment, a double-pass setup is made to obtain interferograms with WYKO. In a real misaligned situation, (a)~(c) of Table 1 are mixed up and often both in X and Y directions, but only the effects in X-direction are shown for simplicity in Table 1.

Table 1. Effect of the secondary mirror alignment component on Zernike coefficients of the telescope

(a) X-Decenter = 0.01 mm

Z1	Piston	-0.0531
[redacted]		
Z3	Y-Tilt	0.0000
Z4	Power	-0.0320
Z5	X-Ast	0.0000
Z6	Y-Ast	0.0000
[redacted]		
Z8	Y-Coma	0.0000
Z9	SA3	0.0188

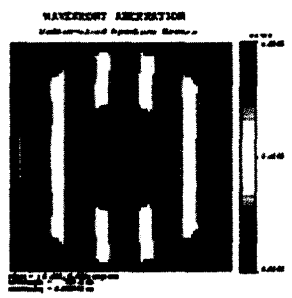

(b) X-Tilt = 0.0167 deg (=1arcmin)

Z1	Piston	0.5956
[redacted]		
Z3	Y-Tilt	0.0000
Z4	Power	-0.0373
Z5	X-Ast	-0.0046
Z6	Y-Ast	0.0000
[redacted]		
Z8	Y-Coma	0.0000
Z9	SA3	0.0200

(c) Z-despace = 0.05 mm

Z1	Piston	-1.2496
Z2	X-Tilt	0.0000
Z3	Y-Tilt	0.0000
[redacted]		
Z5	X-Ast	0.0000
Z6	Y-Ast	0.0000
Z7	X-Coma	0.0000
Z8	Y-Coma	0.0000
[redacted]		

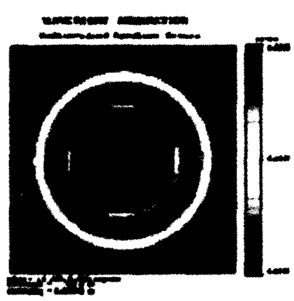

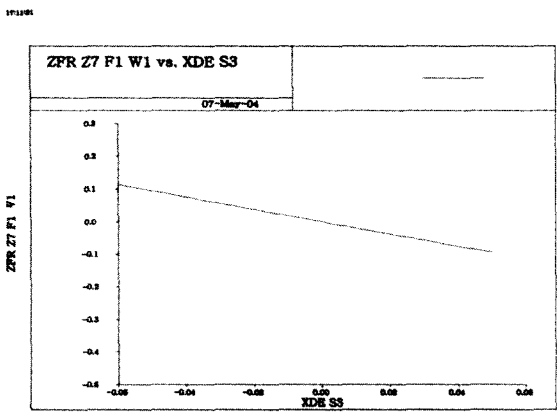

(a) X-decenter vs. X-coma

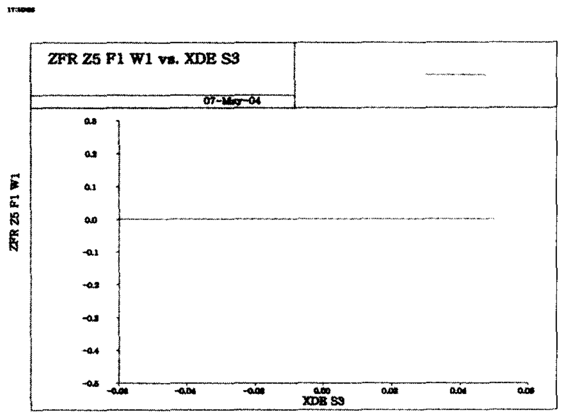

(b) X-decenter vs. 0/90deg astigmatism

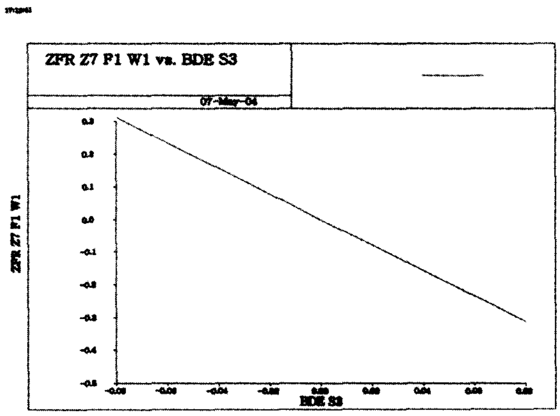

(c) X-tilt vs. X-coma

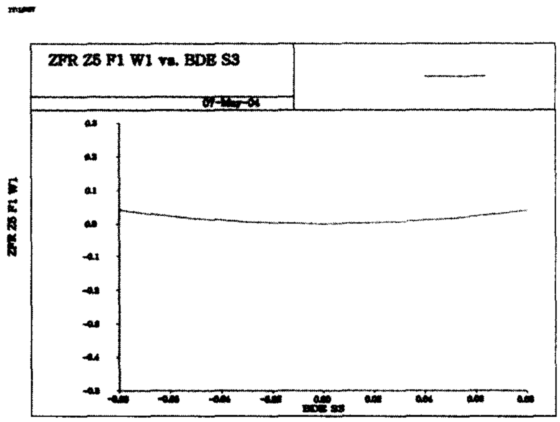

(d) X-tilt vs. 0/90deg astigmatism

Figure 2. X-coma (Z7) and 0/90-deg astigmatism vs. X-decenter and X-tilt (tilt around Y-axis).

By giving typical ranges of decenter (+/-0.06 mm) and tilt (+/-0.08deg=+/-4.8arcmin) to the secondary mirror, the Zernike X-coma (Z7) and 0/90-degree astigmatism (Z5) terms have been checked. Figure 2 shows that Z7 is linear throughout the ranges, and Z5 is slowly changing relative to Z7. It implies that coma is the dominant term when the secondary is closer to an aligned state, and it can be removed by linear combinations of decenter and tilt of the secondary mirror.

From left to right, Figure 3 gives a simulated sequence of Fringe Density Balancing Method. The initial interferogram shows a typical misaligned interferogram in X-direction (also for simplicity). Fringe density on the left and right side of the screen can be balanced in the direction so X-coma coefficient is reduced. After the fringe density is balanced, despace can be adjusted to remove the power and spherical aberration.

However, there is a limit in balancing the fringes, because as the telescope is more aligned, it is more difficult to distinguish the asymmetry in the interferogram. As shown in the interferogram of Figure 3 (c), once it is closer to the aligned state, it is difficult to distinguish the interferogram even though there still remain decenter and tilt. These remained decenter and tilt can be problems for a telescope with large field of view, and they need to be removed. The limit of this method will be discussed again later in the reverse-optimization method section.

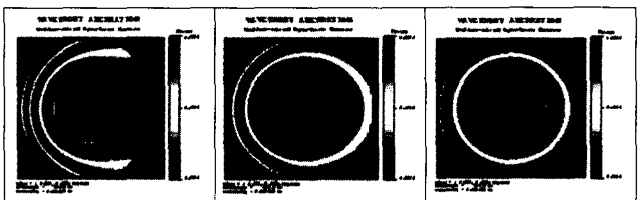

(a)	(b)	(c)
X-Dec=-0.5 mm Y-Tilt=0.0476 deg, Z-Desp=0.05 mm, Z7=0.7582	X-Dec=-0.25 mm Y-Tilt=0.0238 deg, Z-Desp=0.05 mm, Z7=0.3788	X-Dec=-0.05 mm Y-Tilt=0.0047 6deg, Z-Desp=0.05 mm, Z7=0.0757

Figure 3. Simulated Fringe Density Balancing Method for the alignment of M2.

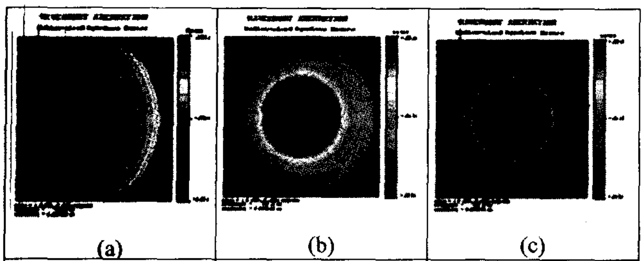

(a)	(b)	(c)
X-Dec=-0.05mm Y-Tilt=0.00476deg, Z-Desp=0.0mm, Z7=0.0757	X-Dec=-0.005mm Y-Tilt=0.000475deg, Z-Desp=0.0mm, Z7=0.0076	X-Dec=0.0mm Y-Tilt=0.0deg, Z-Desp=0.0mm, Z7=0.0000

Figure 4. Simulated OPD Balancing Method for the finer alignment of M2.

In order to tackle this problem, another method but with an identical underlying principle was considered. Despite the ambiguity from the bear fringes, one can further detect the asymmetry in OPD calculated from the interferometer, and hence align the secondary mirror further. This OPD Balancing Method (OBM) is shown in Figure 4 with the simulated sequence of OPDs starting from the last misaligned state from Figure 3 (c). It shows the telescope can be further aligned after FDBM. The advantage of this method is that it does not require OPD measured from different fields of view other the on-axis, but this method needs to be further investigated with experiments.

III. Reverse-optimization method

A current state-of-the-art of alignment method was applied in the final alignment of the Qualification Model of MAC telescope. Conventional alignment method (Figure 5) starts from tolerancing in the design where the alignment compensator *range* is calculated by optical design software. The value of compensator is then decided by an operator while conducting the test. Alignments are made until the test results are satisfactory.

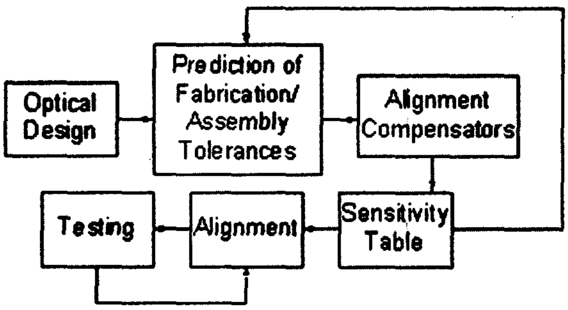

Figure 5. Conventional optical alignment process.

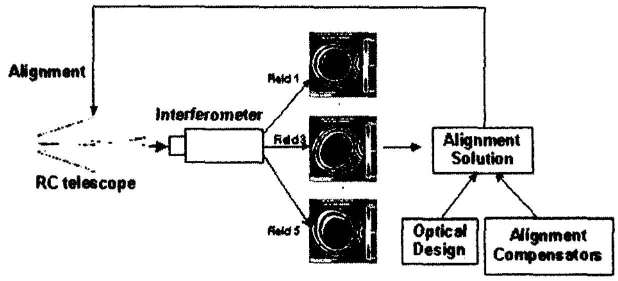

Figure 6. Reverse-optimization alignment method.

However, a reverse-optimization method can give quantitative values of compensators to align the telescope, which can shorten the iterative alignment-test loop. The principle of reverse-optimization alignment method is illustrated in Figure 6. Once the interferograms of a misaligned telescope are taken at different fields of view, Zernike coefficients are extracted from each interferogram, and they are fed back into the optical design program. The compensator values are reversely calculated by minimizing the differences between the as-is Zernike coefficients from the misaligned telescope and those from the theoretically perfectly aligned telescope.

Before applying this method in the alignment experiment, a simulation was done on the design first. A random set of misalignments was given to the secondary mirror and interferograms at different fields were taken inside Code V. The Zernike coefficients extracted from each interferogram were input to the original design and the needed compensator values were calculated. Table 2 shows the simulation result and the method was well verified as the differences were smaller than the measurement precision.

Starting from the last alignment using FDBM, interferograms were taken from five different fields of view as shown in Figure 7 (a). To take the interferograms from different off-axis fields of view, a proprietary interferometer mount was used as shown in Figure 7 (b).

Table 3 summarizes the alignment experiment result using reverse-optimization method. From left to right, each column

Table 2. Simulated reverse-optimization alignment method on MAC

Type	Pert (mm, rad)	Comp (mm, rad)	Diff (mm, deg)
X-DEC	0.131069	0.12989	0.0011787
Y-DEC	0.150247	0.15252	-0.002273
Z-DSPL	0.120394	0.12224	-0.001846
X-TILT	0.002548	0.0025511	-0.000205
Y-TILT	0.001706	0.0017083	-0.000106

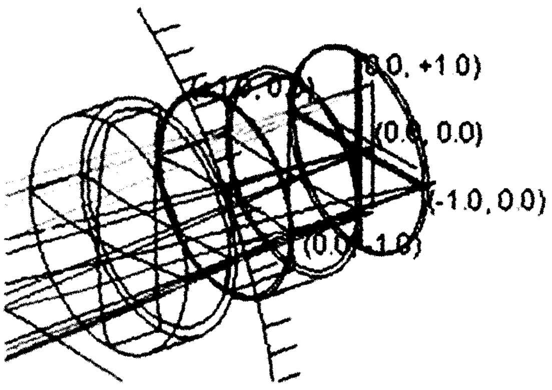

(a)

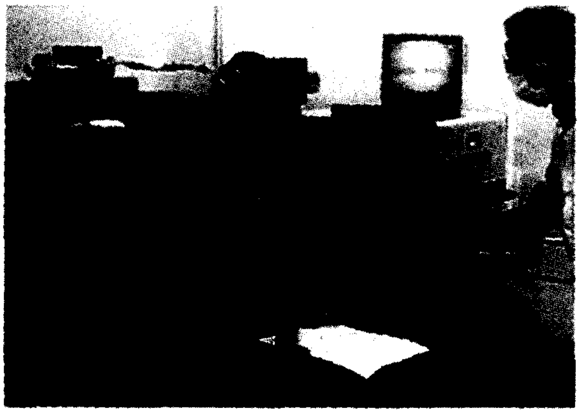

(b)

Figure 7. Five fields of view and proprietary interferometer mount.

Table 3. Alingment experiment result using reverse-optimization method.

Field	Initial	Tilts aligned	Tilts & decenters aligned
(0.0, 0.0)	RMS=70 nm	RMS=102 nm	RMS=63nm
(+1.0, 0.0)	RMS=90 nm	RMS=101 nm	RMS=69 nm
(-1.0, 0.0)	RMS=140 nm	RMS=111 nm	RMS=68 nm
(0.0, +1.0)	RMS=114 nm	RMS=115 nm	RMS=67nm
(0.0, -1.0)	RMS=76 nm	RMS=95 nm	RMS=70nm

shows the OPDs at different fields of view and different stages of alignment process.

The first column shows the stage when the telescope was aligned only with FDBM. Although the on-axis (0.0, 0.0) field shows small RMS wavefront error, other fields are not balanced with visible astigmatism, and hence the usage of FDBM is limited for intial alignment. The second column shows when the tilts of the secondary mirror were corrected, and it now shows some coma in the OPD. When all misalignments are corrected as shown in the last column, very well balanced wavefront error at different fields were measured. It shows the RMS wavefront error lies within 63~70 nm range, and this meets the target of balancing the wavefront errors for different on and off-axis fields.

IV. Conslusion

Different optical alignment methods for different stages of aligning a Cassegrain telescope were investigated. The Cassegrain telescope of a spaceborne earth observation camera was used to verify the methods. Fringe Density Balancing Method (FDBM) and OPD Balancing Method (OBM) were simulated on the actual design of the telescope. FDBM was tried on the MAC Qualification Model (QM) telescope alignment with limited success, where OBM needs to be further tested with more alignment experiments in MAC Flight Model (FM) telescope. Finally, a reverse-optimization method was simulated and successfully applied on the alignment of the MAC QM telescope. It showed that with the reverse-optimization alignment method, we could align the telescope well balanced at different on and off-axis fields with high accuracy. As a further future work, a reverse-optimization alignment method is being considered to align a Three-Mirror Anastigmat (TMA), where it is known to be even more difficult to precisely align the telescope without one.[6]

References

[1] M. Ruda, Fundamentals of Optical Alignment Techniques, (SPIE, Bellingham, US, 1994), pp. 118-124.

[2] D. Li, "Alignment of the optical systems for the 2.16-m astronomical telescope" in Advanced Optical Manufacturing and Testing Technology 2000, L. Yang, *Ed., Proc. SPIE,* vol. 4231, pp. 449-455, 2000.

[3] S. A. Rodionov, et al, "Principles and software for photolithographic optical system alignment and tolerancing" in Optical Design and Analysis Software, R. C. Juergens, *Ed., Proc. SPIE,* vol. 3780, pp. 180-190, 1999.

[4] E-E Kim, Y-W Choi, H-S Yang, et al, "Development of Engineering Model of Medium-sized Aperture Camera System" in 4th International Symposium, *IAA, Berlin, Germany,* pp. 137-144, 2003.

[5] B-J Kim, S-D Park, Ee-Eul Kim, et al, "MACSAT - A Mini-Satellite Approach to High Resolution Space Imaging" in 17th Conf. on Small Satellites, AIAA/USU, Logan, Utah, SSC03-VI-8, 2003.

[6] K. Sugisaki, et al, "Assembly and alignment of three aspherical mirror optics for extreme ultraviolet projection lithography" in Emerging Lithographic Technologies IV, *E. A. Dobisz, Ed., Proc. SPIE,* vol. 3997, pp. 751-758, 2000.

Optical alignment of a high-resolution optical earth observation camera for small satellites

Eugene D. Kim†, Young-Wan Choi, Myung-Seok Kang, and Ee-Eul Kim

Satrec Initiative, 461-26 Jeonmin-dong, Yuseong-gu, Daejeon 305-811

† *E-mail: edk@satreci.com*

Ho-Soon Yang

Korea Research Institute of Standards & Science, 1 Doryong-dong, Yuseong-gu, Daejeon, 305-600

(Received May 13, 2004, Revised manuscript July 5, 2004)

Spaceborne earth observation or astronomical payloads often use Cassegrain-type telescopes due to the limits in mass and volume. Precision optical alignment of such a telescope is vital to the success of the mission. This paper describes the simulated optical alignment methods using interferograms, wavefront error, and reverse-optimization method for different levels of alignment accuracy. It concludes with the alignment experiment results of a Cassegrain type spaceborne camera with 300mm entrance pupil diameter.

OCIS Codes : 350.6090, 110.6770.